

Velocity and Concentration Measurements in Initial Region of Submerged Round Jets in Stagnant Environment and in Coflow

L. P. Xia¹ and K. M. Lam²

Abstract: Velocity and concentration fields are measured in submerged round jets in a stagnant environment and in coflow using laser-Doppler anemometry and laser-induced fluorescence. Measurements are made in the initial region within distances of 40 jet exit diameter at jet Reynolds number between 1,000 and 5,000 and coflow-to-jet velocity ratio from 0 to 0.43. Different behaviors of jet spreading and dilution are found in jets at three different ranges of Reynolds number in which the jets are classified as initially laminar, transitional or turbulent. In the zone of established flow, the jet centerline velocity and concentration decay with downstream distance at different rates in the three groups of jets. For jets in coflow, axial development of normalized forms of centerline mean excess velocity and mean concentration at different velocity ratios can be reasonably well collapsed onto universal trends through the use of momentum length scale. Turbulence properties inside a jet are increased by the presence of a strong coflow. Inside the zone of flow establishment, some strange features are observed on jet turbulence properties. The length of zone of flow establishment increases from the turbulent jets, to the transition jets and to the laminar jets. The zone lengths for concentration are shorter than those for velocity by one to two jet exit diameters. Both lengths are shortened further in the presence of a coflow. For jets a stagnant environment and in the strong jet flow region of jets in coflow, jet widths increase linearly with downstream distance in transitional and turbulent jets. Self-similarity of radial profiles of mean velocity or excess velocity, mean concentration, turbulence intensities and concentration fluctuation level is explored in the zone of established flow.

1. Introduction

Mixing and dilution capabilities of a submerged round jet are important in many engineering and hydraulic applications involving discharge of jet effluent into an ambient fluid. Extensive measurement data of mean velocity and statistical turbulence properties have been reported in the literature (e.g., Rajaratnam 1976, Fischer et al. 1979, Wood et al. 1993, for review). The decay rate of mean jet centerline velocity and the growth rate of jet width are usually analyzed to indicate the efficiency of jet spreading and mixing. Changes of these jet properties occur in the zone of established flow (ZEF) where self-similarity is being achieved for many flow quantities, in particular the radial velocity profiles. Relatively fewer measurements have been made on the zone of flow establishment (ZFE), also known as the potential core, of the jet.

In addition to flow velocities, measurement of concentration field of jet effluent is equally important in determining the spreading and dilution of a jet. Early experimental studies employed probe-based single point measurements by change in conductivity, temperature or light absorption by dye. The amount of data was far less extensive than velocity data and limited mostly to discharge of buoyant jet effluent. Introduction of laser-induced fluorescence (LIF) technique has resulted in increasing numbers of jet experiments with concentration measurements and data (e.g., Papantoniou and List 1989, Davidson and Pun 1999). It is found that along the jet centerline, the mean concentration starts to drop earlier than flow velocity and that the concentration jet width is larger and grows faster than the velocity jet width.

Initial jet exit conditions and jet Reynolds number have been found to affect development of a round jet (Xu and Antonia 2002, Kwon and Seo 2005). At low Reynolds numbers (Re), roughly lower than 1,000, the jet is laminar and Kwon and Seo (2005) found a number of flow behaviors different from a turbulent jet at high Re . For instance, the ZFE has a length longer than the turbulent jet value of 6.2 jet exit diameters and the rate of drop of centerline velocity does not follow that $-1/x$ relationship as a turbulent jet (x being the downstream distance from the jet exit).

Spreading and mixing of a round jet is affected by the presence of a main flow in the ambient fluid. Among all possible relative directions of jet exit to the moving ambient, the coflow and crossflow situations have been studied most. A coflowing jet is found to have two asymptotic regions; a strong jet region near to the jet exit and a downstream weak jet region where magnitudes of local velocities in the jet become comparable to the ambient flow velocity (Antonia and Bilger 1973, Davidson and Wang 2002).

This paper reports results of our experiments on a number of round jets at different Reynolds numbers in stagnant ambient and in coflow of different ambient flow velocities. Non-intrusive laser-based measurement techniques are adopted: laser Doppler anemometry (LDA) for velocity measurement and LIF for concentration measurement. The main purpose is to provide spreading and mixing data of in ZFE of simple jets (that is jet in a stagnant environment) and jets in coflow under a wide range of Re and coflow strengths. Our emphasis is on relative low Re in the order of thousands. Past experimental works were mostly related to industrial applications and were performed at high Re above 10,000. However, low Re jets are relevant to a wide range of flows in environmental and biological applications and have received more frequent attention in recent years (Zarruk and Cowen 2008). We attempt to test the similarity behavior of the jet at the different ranges of Re and coflow strengths. Our measurements are made in the initial region of the jet within an axial distance of 20 to 40 jet exit diameters. This initial near-field region and the ZFE have received less attention in previous studies and few measurement data are available on the transition to self-similarity which occurs here.

2. Experimental Setup

The experiments were carried out in Croucher Laboratory of Environmental Hydraulics at The University of Hong Kong. The main flow apparatus was a laboratory flume with a 10 m long and 0.3 m wide flow section. To produce a coflow, horizontal flow of speed U_o up to about 0.2 m/s was maintained in the flow section by recirculating water. Variations and fluctuations of flow speeds in the flume had been measured with LDA. The variation of axial flow velocities within the central part of the flow section was less than 3% while the turbulence intensity at mid-depth was about 5%. In the simple jet

experiments, water was kept stagnant in the flume by installing gates at two ends of the flume. Water depth was kept at about 0.35 m in all experiments. A submerged round jet was formed by discharging water into the flume from a circular nozzle fed from a constant overhead tank. The nozzle had an exit diameter $D = 3$ mm and was placed at mid-depth of the flume. To ensure clean initial exit conditions, the nozzle was preceded by a 4:1 contraction section and there was a parallel flow section of length $2D$ before jet exit. The jet exit velocity U_j was set with a flow valve at value between 0.3 m/s and 1.5 m/s.

The mean jet flow field was axisymmetric. Axial and radial flow velocities were measured with a two-component fiber-optic LDA along the jet centerline and at a number of jet sections. Measurements along jet centerline covered a distance from 0 to $40D$ with resolution ranging between $0.5D$ and $1.5D$. Measurements across jet sections were made within radial distances from $-4D$ to $4D$ and spatial resolution ranged between $0.3D$ and $0.5D$. At each measurement point, velocities were measured for 1 min. to obtain the mean velocities and statistical turbulence quantities such as turbulence intensities and Reynolds stresses.

In LIF measurements, fluorescent dye Rhodamine 6G was added to jet effluent in the overhead tank at a constant concentration. The laser beam from a 4-watt Argon-ion laser was turned into a laser sheet with a triangular lens. The laser sheet cut through the central vertical plane of the jet. A high-speed CCD-camera of resolution $1028 \text{ pixel} \times 672 \text{ pixel}$ recorded LIF images at 50 images/s. For each test flow condition, 500 LIF images were recorded. The initial time scale of the jet was estimated by D/U_j to be of the order of ms and as the jet spread downstream, the time scale would become longer. The sampling period of 10 s was considered sufficiently long to capture the mean jet behaviors. Calibration of the LIF system had been carried out with known concentrations of Rhodamine 6G from 0.005 to 0.065 mg/L. Thereafter, concentration field of fluorescence dye in the jet flow could be determined from the gray values in the LIF images.

Some LIF experiments on jet in coflow were carried out in a water basin with the equivalent situation of towing the jet nozzle in otherwise stagnant water (Davidson and Wang 2002). In the present study, the towed jet experiments were carried out in a basin of length 12 m and width 5 m. It was filled with water to about 0.8 m and the jet nozzle was

towed with a computer-controlled table along the length of basin. Flow images were taken with the CCD camera which was towed together with the jet nozzle.

3. Experimental Conditions

The different flow conditions tested are listed in Table 1 for LDA and Table 2 for LIF measurements. The main flow parameters being varied were the jet Reynolds number $Re = U_j D / \nu$, and the relative strength of coflow as measured by the coflow-to-jet velocity ratio, $R = U_o / U_j$. Reynolds numbers of jets covered a range between $Re = 1,000$ and $5,000$ roughly. Although it is commonly accepted that most jet flows will be turbulent if Re exceeds $2,000$, the value of Re at which a laminar jet becomes turbulent depends on many factors including initial jet conditions and the transition is gradual. As shown in Tables 1 and 2, we have classified our jets into three groups: laminar jets at $Re \approx 1,000$, transitional jets at $Re \approx 1,600$ to $1,700$ (and one jet at $Re = 2,500$), and turbulent jets at $Re \approx 3,300$ to $3,500$ (and two higher Re jets at $Re \approx 5,000$). For jets in coflow, the coflow-to-jet velocity ratio (velocity ratio for short) ranged from $R = 0.008$ to 0.430 .

Fig. 1 shows the mean velocity profiles near the jet exit of a turbulent jet at $Re = 3,405$ and a transitional jet at $Re = 1,744$. The exit velocity profile of the turbulent jet departs from the perfect top-hat distribution due to the boundary layer effect after the small contraction ratio and a parallel section in the jet nozzle. However, it is evident that the transitional jet has a distinctly different exit velocity profile which is closer to the parabolic distribution. The laminar jet at $Re = 1,027$ possesses velocity profiles very similar to those of the transitional jet in Fig. 1(b) and the data are not shown for brevity.

4. Results and Discussion

4.1. Centerline Flow Quantities in Simple Jet

For a turbulent round jet, it is commonly accepted that the centerline velocity decays with $-1/x$ in the self-preserving ZEF as:

$$\frac{U_c}{U_j} = \frac{L - x_0}{x - x_0} = \frac{C_1}{(x - x_0)/D} \quad (1)$$

where x_0 is distance of virtual origin of the jet from jet exit. Length L of the ZFE or potential core is a multiple of jet exit diameter and this multiple C_1 is also described by some workers as the decay constant (Hussein et al. 1994, Antoine et al. 2001, Xu and Antonia 2002). In hydraulic applications, length of ZFE in a simple jet is usually assumed at $L = 6.2D$. Investigations on air jets find a value of C_1 about 6.5 or higher for ideal jets with an initial top-hat velocity profile and a value of C_1 between 5.6 ~ 5.9 for jets with an initial parabolic velocity profile similar to one inside a pipe (Xu and Antonia 2002). Not all past studies chose to use the virtual origin x_0 in the data fitting of $U_c(x)$, and when it is used, values ranging from 0 to $5D$ have been obtained (Antoine et al. 2001). In a recent numerical study of jets in coflow, the virtual origin is argued to play a significant role in describing the self-similarity behavior of the jet (Uddin and Pollard 2007).

For the test runs in Table 1, time-averaged mean axial flow velocities along the jet centerline, $U_c = U_c(x)$, have been measured with LDA. The results clearly show that jets at different ranges of Re exhibit different decay behaviors of $U_c(x)$ in ZEF. Figs. 2(a-c) show the data of U_c/U_j against x/D , respectively for the three groups of jets. One evident observation is that in the laminar jets, the centerline velocity starts to drop from the jet exit value at the longest distance among the three groups of jets, that is, they have the longest ZFE lengths. The turbulent jets have much shorter ZFE lengths.

Our turbulent jets in Fig. 2(a) show the expected decay rate of $U_c \sim x^{-1}$ in the ZEF. However, the lengths of ZFE are not quite consistent with those in the literature. For the two turbulent jets at $Re \approx 3,300$ to $3,400$, the ZFE length, as determined from the distance at which U_c starts to decrease, is about $L/D \approx 5$ to 6 . The jet at a higher $Re \approx 5,000$ shows an even shorter L . Kwon and Seo (2005) recently reported velocity data of simple round jets at similar values of Re and data of their two jets are included in Fig. 2(a). Their data and our jet at $Re \approx 5,000$ show that $U_c(x)$ starts to drops from U_j as early as $x \approx 4D$ to $5D$. A value of $L/D = 5.5$ is obtained from the fitting of all turbulent jet data. Fig. 2(b) shows the centerline velocity data for the group of jets classified as transitional jets. There are two jets at $Re \approx 1,700$ and one jet at a higher $Re \approx 2,500$. The decay of U_c with x in ZEF is better described by the $x^{-4/3}$ relationship than x^{-1} . The lengths of ZFE of these transitional

jets are clearly longer than those of the turbulent jets. The centerline velocity starts to drop at $x/D \approx 6$ while the decay slope at $-1.33/x$ gives a value of $L/D = 7.0$. Data of Kwon and Seo (2005) for a jet at $Re = 2,163$ are also included. Although their data lie clearly above our curve, they follow approximately our decay slope. Our last group of jets in Fig. 2(c) includes some laminar jets at $Re \approx 1,000$. The centerline velocity starts to drop after a much longer ZFE at $x \approx 7D$. Data of a jet in Kwon and Seo (2005) at $Re = 1,305$ are included. No well-defined relationship can be found for the decay of centerline velocity for this group of laminar jets. In the first part of ZEF roughly at $x/D < 20$, the data can be roughly described by the $x^{-1.5}$ relationship but farther downstream, decay rate of $U_c(x)$ clearly becomes slower. The length of ZFE as obtained from the $x^{-1.5}$ decay is $L/D = 9.0$. Kwon and Seo (2005) reported similar observations of longer ZFE lengths and different centerline velocity decay behaviors at low Re but that study did not fit the data to any equation.

In many past studies, the development of centerline velocity was plotted in the form of U_j/U_c against x in order to determine the values of C_1 and x_0 in Eq. (1). We have taken this approach to analyze our data of $U_c(x)$ in Fig. 2 and the resulting values of C_1 and x_0 (rounded off to $0.5D$) for the three groups of jets are listed in Table 3. The turbulent jets have a very small virtual origin but for the $U_c(x)$ data of the transitional and laminar jets to follow the x^{-1} decay, a virtual origin at $x_0 = 2.5D$ and $4.5D$ needs to be applied respectively. The curves of Eq. (1) with the values of C_1 and x_0 in Table 3 are plotted in Fig. 2. For the transitional jets and laminar jets in Figs. 2(b-c), the curves are different from the previously fitted curve of $U_c \sim x^{-4/3}$ and $U_c \sim x^{-1.5}$, respectively. It appears that the inclusion of a virtual origin results in better description of the data.

Past studies have found that the decay constant C_1 (the ZFE length) of a turbulent round jet can vary over a range of values depending on factors including initial velocity profiles, nozzle shapes, and amount of flow entrainment near jet exit (Antoine et al. 2001, Xu and Antonia 2002, Babu and Mahesh 2004, Quinn 2006). Our turbulent jets give a value of $C_1 = 5.5$ which is shorter than the commonly accepted value of 6.2. Nevertheless, it is evident both from the power decay fitting and from Eq. (1) with the inclusion of x_0 that the ZFE has significantly increasing lengths as the jet changes from turbulent to transitional, and to laminar. This observation is also partly made on Fig. 1 in which U_c in

the velocity profile of the turbulent jet at $x/D = 6$ clearly drops from the jet exit value when U_c in all velocity profiles of the transitional jet at $x/D \leq 6$ still remain at the exit value.

LIF measurements have been made on simple jets at $Re = 1,003, 1,672, 3,345$ and $5,017$ (Table 2). Mean LIF images are obtained from the ensemble of LIF images of these jets. It is clearly observed from the mean LIF images that the length of ZFE in the laminar jet is the longest among the four jets while the turbulent jet at the highest Re has the shortest ZFE length. This ZFE length, L_T , which refers to the tracer or concentration field, is different from the ZFE of the velocity field. Concentration data are extracted from the mean LIF images and Fig. 3 compares downstream development of centerline concentration in our simple jets at different Re . Previous studies, mostly based on measurements of jets at high Re , suggested that centerline concentration remains unchanged at C_j inside L_T and then decays with the power of x^{-1} in the ZEF:

$$\frac{C_c}{C_j} = \frac{L_T - x_0}{x - x_0} \quad (2a)$$

$$\text{or } \frac{C_j}{C_c} = \frac{1}{(L_T - x_0)/D} \left(\frac{x}{D} - \frac{x_0}{D} \right) \quad (2b)$$

Here, C_c is the centerline concentration and C_j is the scalar concentration at jet exit. We have plotted our data of C_j/C_c against x/D and thus determined the values of L_T and x_0 . These values are rounded off to $0.5D$ and listed in Table 3 for the three groups of jets. It is worth noting that the virtual origin for scalar concentration can have a different value from that for the centerline velocity. In Fig. 3, we choose to multiply the normalized concentration level C_c/C_j by Re before plotting against x/D to show the effect of Re . It is evident that with the inclusion of the right value of x_0 , the centerline concentration can be described well by Eq. (2a). For the transitional and turbulent jets, the virtual origin has negative values, that is, located upstream of the jet exit. The existence of a negative virtual origin has been observed in some experiments and a plausible explanation was recently discussed in Uddin and Pollard (2007). In the LIF experiments of Antoine et al. (2001) at $Re = 10,500$, the centerline concentration decay also gave rise to a negative virtual origin at $x_0 = -11D$.

From Fig. 3 and Table 3, the tracer ZFE is found to have the longest length in the laminar jets ($L_T = 9.5D$) and the shortest in the turbulent jets ($L_T = 4.5D$). For the

transitional jets, the length is $L_T/D = 5.5$. Except for the laminar jets, the tracer ZFE lengths are shorter than the ZFE length of the velocity field by $1D$ to $1.5D$. In terms of the rate of concentration decay with axial distance downstream of ZFE, the decay rate of the laminar jet is clearly faster than the other two groups of jets at higher Re .

4.2. Centerline Flow Quantities of Jet in Coflow

Fig. 4 shows the drop of jet centerline velocity with axial distance x/D for the three groups of jets in coflow: initially laminar, transitional and turbulent jets. To show the effect of Re , jet centerline velocity data are shown as $U_c D/\nu$. In each group of jets, centerline velocity drops towards ambient flow velocity U_o in the ZEF. In a coflow of small R , the drop of $U_c(x)$ follows approximately the same slopes as the simple jets. These slopes of $x^{-1.5}$, $x^{-1.33}$ and x^{-1} found for the three groups of simple jets are plotted in Fig. 4. However, in order to fit the data, the decay constant, which also means the ZFE length, needs to be lowered accordingly. In the turbulent jets, this ZFE length decreases from $L/D = 5.5$ in the stagnant environment to $L/D = 4.5$ in a coflow. Shortening of ZFE in a coflow in transitional jets is from $L/D = 7.0$ to 5.0 and in laminar jets, from $L/D = 9.0$ to 6.0 .

Alternatively, We also try to fit the x^{-1} decay to all groups of jet with the inclusion of virtual origins. The values of x_0 in Table 3 for the simple jets are used while the decay constant C_1 is adjusted to fit the data in Fig. 4. As shown in the figure, the curves of x^{-1} provide a lower envelope to the data. For the transitional jets with $x_0 = 2.5D$, the values of C_1 become lowered from 4.5 to 3.0 . For the laminar jets with $x_0 = 4.5D$, C_1 decreases from 4.5 to 2.5 . When combined with the values of x_0 , the lengths of ZFE are $4.5D$, $5.5D$ and $7.0D$, respectively for the turbulent, transitional and laminar jets. These ZFE lengths are lower than those values for the simple jets by $1D$ to $2D$ (Table 3). The finding suggests that the ZFE of a jet ends earlier in a coflow than in stagnant ambient.

For a jet in coflow, mixing is believed to be driven by flow velocities in the jet in excess of the ambient coflow velocity. Thus, a longer ZFE is commonly expected in a coflowing jet due to the smaller velocity shear in the presence of a coflow (Chu et al. 1999). Our present observation of shortening of ZFE in a coflow seems questionable. However, direct numerical simulation of Babu and Mahesh (2004) found that the potential

core of a simple jet closes earlier when there is a coflowing stream around the jet. They argued that the shorter ZFE length is due to inflow entrainment near the jet exit. For a subsonic air jet in coflow, Burattini et al. (2004) also reported a short length of $L = 4D$ for the potential core. For a plane jet in a shallow coflow, Gaskin et al. (2004) suggested that background turbulence reduces dilution yet it was also pointed out that the effect of background turbulence on the near-field dilution is not straightforward. On the other hand, it is tempting to argue that turbulence intensity at about 5% in the ambient coflow generated in our flume may be responsible for an earlier erosion of jet potential core and thus leading to a shorter ZFE. A coflow of almost zero turbulence level can be simulated by towing a jet (Davidson and Wang 2002) but it is difficult to measure flow velocities in this situation. We have made LIF measurements on the towed jet situation with results to be presented in later sections. It will be shown that there are no significant differences in the global behavior of jet in coflow between our flume experiments and towed jet experiments. However, the effect of background turbulence on initial jet development remains to be unresolved.

Length scale analysis is often used to study jets and plumes in a moving environment (Woods et al. 1993). For a jet in coflow, the governing length scale is the excess momentum length scale l_m . It is defined as the ratio:

$$l_m = M_e^{1/2} / U_o \quad (3)$$

where $M_e = (U_j - U_o) U_j \frac{1}{4} \pi D^2$ is the initial excess momentum of the jet at exit. Value of l_m represents the distance at which advection effect of the coflow becomes important in the flow of jet effluent (Davidson and Wang 2002). In the jet near field, effect of coflow is small and the jet behaves similarly to a jet in stagnant ambient with centerline velocity decaying as x^{-1} . At large distances from jet exit, where $x \gg l_m$, jet effluent is mostly advected by the coflow and the centerline velocity follows the $x^{-2/3}$ decay (Fischer et al. 1979).

The drop of jet centerline velocity from the exit value to the ambient coflow value is usually studied using the centerline excess velocity, $U_{ec}(x) = U_c(x) - U_o$. To collapse data of jets at different velocity ratios, Fig. 5 shows the normalized curves of excess velocity along jet centerline in the form of U_{ec}/U_o against $(x-x_0)/l_m$. Our measurement region is

within $(x-x_0)/l_m < 10$ and the coflowing jets are expected to behave like a strong jet (Davidson and Wang 2002). However, different behaviors are found in our three groups of jets. For turbulent jets at $Re \approx 3,300$ and velocity ratios R between 0.008 and 0.121, our data of U_{ec}/U_o in ZEF, within $x/l_m < 10$, follow nicely the decay with x/l_m to the power -1 (Fig. 5a). For our initially transitional jets, the data of U_{ec}/U_o do not vary nicely with $(x/l_m)^{-1}$. However, when we include the effect of the virtual origin, the drop of U_{ec}/U_o with $(x-x_0)/l_m$ is found to better follow the -1 power law (Fig. 5b). For the decay of centerline excess velocity in our initially laminar jets, the $-1/x$ decay only applies to the jets at lower velocity ratios and within $(x-x_0)/l_m < 1$, even after the inclusion of x_0 (Fig. 5c). For jets at larger R and beyond $(x-x_0)/l_m \geq 1$ in all jets, the decay of U_{ec}/U_o with $(x-x_0)/l_m$ occurs at a much faster rate.

For jets in coflow, downstream development of centerline concentration can be expressed as the velocity-ratio-weighted centerline dilution, that is $S_c R/(1-R)$, where $S_c = C_j/C_c$ is the dilution at jet centerline (e.g., Chu et al. 1999). Fig. 6 plots this normalized centerline dilution against x/l_m for our three groups of jets in Table 2. Previous studies have suggested a linear relationship between $S_c R/(1-R)$ and x/l_m as:

$$S_c(x) \frac{R}{1-R} \approx k \left(\frac{x}{l_m} \right) \quad (4)$$

Values between 0.16 and 0.18 have been found and suggested for the proportionality constant k (Chu et al. 1999, Davidson and Wang 2002). In analyzing our concentration measurement, we find that inclusion of the virtual origin leads to a better collapse of data in the initial region of the jet. In Fig. 6(a), our dilution data of turbulent jets at $Re = 3,345$ follow nicely Eq. (4) but with a constant of value on the low side at $k = 0.16$. A negative virtual origin at $x_0 = -2.5D$ has been included in the abscissa. Results from two towed jet experiments at the same Re are included in the figure and the dilution data do not show any remarkable difference from those of the flume experiments. Fig. 6(b) shows centerline dilution for the laminar and transitional jets as well as a towed jet at $Re = 1,672$ and $R = 0.05$. Most jets in the figure behave similarly in their dilution behavior and are described well by Eq. (4). The exceptions are the laminar jets in a strong coflow at $R > 0.2$. Those jets also exhibit some particular trends of centerline velocity decay in Fig. 5(c).

4.3. Jet Widths and Radial Profiles of Velocity and Concentration

Velocity measurements have been made across many jet sections in a number of transitional and turbulent jets including simple jets and jets in coflow. Those test cases are marked with an asterisk in Table 1. In ZEF of a simple jet, radial profiles of mean axial velocities $U(x,r)$ have been found similar and can be described by the Gaussian distribution:

$$U(x,r) = U_c(x) \exp\left[-(r/b)^2\right] \quad (5a)$$

where r is the radial distance and $b = b(x)$ is the (Gaussian momentum) jet width. For a jet in coflow, similarity of radial velocity profiles is expected on the excess velocity, that is $U_e(x,r) = U(x,r) - U_o$, after normalized by the maximum value, $U_{ec}(x) = U_e(x, 0)$, on the jet centerline. The similarity is also described by the Gaussian distribution:

$$U_e(x,r) = U_{ec}(x) \exp\left[-(r/b)^2\right] \quad (5b)$$

Fig. 7 shows the normalized radial profiles of mean axial excess velocity in ZEF of jets in coflow. Jet sections are within $8 \leq x/D \leq 20$. Self-similarity of these normalized excess velocity profiles is observed quite well in the turbulent jets in Fig. 7(a). Data of a turbulent simple jet are included in the figure and it is observed that presence of a coflow does not alter the similarity Gaussian form of radial velocity profiles. Results of initially transitional jets including one simple jet and five jets in coflow are shown in Fig. 7(b). Self-similarity to the Gaussian of these radial excess velocity profiles is not as good as that in the turbulent jets.

From the similarity profiles, Gaussian jet widths b at different jet sections are found as the radial location where $U_e/U_{ec} = 1/e$. These widths are momentum jet widths and they have used to normalize the radial coordinates in Fig. 7. The axial development of these jet widths is shown in Fig. 8 for all three turbulent jets and five transitional jets in coflow. Both jet widths and axial distances are normalized by the excess momentum length scale l_m of individual jets. Data of all jets at different values of R are found to fall on a single curve of growth. A linear growth of jet width has been found in many studies on the simple jet and the average slope value from many data is $k = 0.107$ (Fischer et al. 1979), that is:

$$b/l_m = k(x/l_m) = 0.107(x/l_m), \quad x \ll l_m \quad (6)$$

Eq. (6) is included in Fig. 8 and it provides an upper bound to our data at $x/l_m < 1$. A linear growth of jet width is also found on our two simple jets, data of which are not shown for brevity. In Fig. 8, we have not included the virtual origin x_0 in the abscissa. When the values of x_0 in Table 3, which have been obtained from the centerline velocity decay of the simple jet, are used, the jet width data of the transitional jets would be shifted away from the observed trend in Fig. 8. It is noted that in the literature where the virtual origin is used in the growth of jet widths, two forms of relationship, $b \sim (x-x_0)$ and $b \sim (x+x_0)$, have been suggested (Kwon and Seo 2005, Quinn 2006). It is also unclear whether the same value of x_0 should be applied to the centerline velocity decay and the growth of jet width. Here, we choose not to apply any value of x_0 for the axial development of these momentum jet widths as well as for the concentration jet widths to be presented later.

For jets in coflow, Davidson and Wang (2002) analyzed jet width data from many experimental studies and showed that when flow velocities in the jet are strong compared to the coflow, jet width increases linearly with x but when jet flow velocities are weak, b varies with $x^{1/3}$. A closer observation at their results shows that the jet width data fall well on the asymptote $b \sim x$ at $x/l_m < 1$ and collapse onto the asymptote $b \sim x^{1/3}$ at very large values of $x/l_m > 20$ roughly. The latter asymptotic curve provided in Davidson and Wang (2002) is included in Fig. 8. Our LDA measurements of this paper do not extend to values of x/l_m beyond 10 but it is expected that jet widths far downstream will approach the asymptotic curve.

Radial profiles of mean concentration have been extracted from the mean LIF images of our simple jets and jets in coflow. It is found that the radial concentration profiles across jet sections in the ZEF (not shown for brevity) are found reasonably self-similar to the Gaussian distribution:

$$C(x, r) = C_c(x) \exp\left[-(r/b_r)^2\right] \quad (7)$$

Similar to LDA results, self-similarity to the Gaussian is the best for turbulent jets, good for transitional jets but not so good in laminar jets. Presence of a coflow, of varying strengths, does not seem to alter the self-similar behavior of radial concentration profiles.

Data of jets in coflow from two towed jet experiments are also available and they show no difference from those of the flume experiments.

The width b_T is the concentration (tracer) jet width and many studies have suggested that it is proportional to the momentum width by a fixed ratio: $b_T = \lambda b$ (Fischer et al. 1979, Chu et al. 1999, Davidson and Wang 2002). The generally accepted value of λ for a simple round jet is between 1.1 and 1.4 and it has been suggested that the same ratio applies to jets in coflow. Fig. 9 shows the growth of b_T with x in our simple jets. For turbulent jets, result at a higher Re jet at $Re = 5,017$ is included with the one at $Re = 3,345$. Similar to past studies, a linear growth is observed in our transitional and turbulent jets at a rate of $b_T/x = 0.12$. With the results in Fig. 8, this suggests a value of $\lambda = b_T/b = 1.12$. Data of the laminar jet do not fall well on the linear growth curve and the jet clearly spreads with a larger rate in the region $10 < x/D < 30$. This different behavior of the laminar jet seems consistent with its faster decay curve of $C_c(x)$ in Fig. 3. As described earlier, the effect of virtual origin of the jet is not included in Fig. 9 and the later Fig. 10.

For jets in coflow, Fig. 10(a) shows the growth of concentration jet widths for our transitional and turbulent jets. The momentum length scale l_m is used to normalize both distances to collapse data at different velocity ratios onto a similar trend. The collapse of data for our jets is not good but a general growth trend of jet width can be observed. Similar to the momentum jet width data in Fig. 8, there is approximately linear growth of b_T with x in the strong jet flow region at $x/l_m < 1$, with the same growth constant at 0.12 as the simple jet. Farther downstream when the coflow starts to exert its effect on the jet flow, b_T grows with a slower rate with x . Also included in Fig. 10(a) are data of two turbulent jets in towed jet experiments. Previous results of Knudsen (1998) and Chu et al. (1999) are added in the figure and they fall well onto our data. At large values of x/l_m , effect of the coflow becomes more significant and the flow transits into the weak jet flow regime in which the jet width has been shown to vary with $x^{1/3}$ (e.g., Davidson and Wang 2002). Fig. 10 shows that the present data of b_T will approach the asymptotic curve of the weak jet beyond $x/l_m > 20$.

Jet width data of our laminar jets at $Re = 1,003$ are shown in Fig. 10(b). Similar to the observation on the simple laminar jet in Fig. 9, b_T clearly does not increase linearly with x in the more upstream part of ZEF. Farther downstream at larger values of x/l_m , the growth

of b_T with x follows better the expected growth trends. This implies that jet flow in this region has become independent of the initial jet exit conditions and the jet effluent with low excess velocities is being purely advected by the coflow.

4.4. Turbulence Quantities

Our LDA measurements also include turbulence velocity properties including standard deviations of axial velocity fluctuations, u' , and Reynolds shear stress, $\overline{u'v'}$. Fluctuations of the radial velocity component are measured as well but are not reported for brevity. Fig. 11 shows the radial distributions of axial turbulence intensity in the ZEF of some of our simple jets and jets in coflow. The jet sections shown are within $8 \leq x/D \leq 20$. Turbulence intensity is computed as u'/U_c or u'/U_{ec} . For a simple jet, similarity has been reported on $u'(r)/U_c$ in ZEF and the recent measurement results of Webster et al. (2001) are added in the figure. Turbulence intensity data of our turbulent simple jet, and our transitional simple jet (not shown for clarity), are found to exhibit reasonable degree of self-similarity when plotted against r/b . Data of two turbulent jets in coflow at $R < 0.1$ also fall onto those of the simple jets. The similarity form of our data agrees with that of Webster et al. (2001) on the outer part of the jet but has lower values of turbulence intensity in the inner part at $-1 < r/b < 1$. It was, however, pointed out in Webster et al. (2001) that the axial turbulence intensity values at the centerline vary between 0.24 and 0.3 in the literature and their data are on the higher side. In a stronger coflow, data of our turbulent jet at $R \approx 0.2$, not shown, lie obviously above data of the simple jet and jets in weaker coflow. The same departure is observed on all transitional jets in a coflow even from the lowest velocity ratio at $R = 0.016$. It seems that presence of a coflow leads to increase in the turbulence intensity of a jet in the ZEF and that the turbulent jets, as compared with transitional jets, are less affected by the coflow. One may query that the increase in turbulence intensity is due to turbulence level in our ambient coflow produced in the flume. We could not carry out LDA experiments in a towed jet situation to investigate this possibility which remains unresolved. However, the different behaviors between transitional and turbulent jets could not be explained with the effect of ambient turbulence in the coflow.

The radial distributions of Reynolds shear stress are shown in Fig. 12. The stress is normalized by the square of centerline jet velocity or jet excess velocity. Similar to the observations on axial turbulence intensity, presence of a coflow is found to increase the magnitudes of $\overline{u'v'}/U_c^2$ or $\overline{u'v'}/U_{ec}^2$ except for a turbulent jet at a low value of $R < 0.2$. In jets where Reynolds stress is not significantly increased by the coflow, the data agree with those far-field data of Webster et al. (2001). Peak values of shear stress at $\overline{u'v'}/U_c^2 \approx \pm 0.025$ occur near $r/b \approx \pm 0.6$. Reynolds shear stress is produced by large-scale fluid rotations induced by the coherent structures of the jet. It should not be affected by the ambient turbulence level in the coflow. This is why Reynolds stress has zero value outside the jet. Thus, results in Fig. 12 may help to exclude the possibility that the ambient turbulence level in the coflow is responsible for an apparent increase of u' and $\overline{u'v'}/U_c^2$ in the jet.

Near the jet exit and in ZFE of the jet, the jet potential core with jet exit velocity is being eroded away with the growth of the annular shear layer from the nozzle edge. Turbulence is produced in the shear layer and a peak is produced there in the radial profiles of u'/U_j . The effect of coflow strength R on the turbulence intensity inside ZFE is shown in Fig. 13 by plotting radial profiles of u'/U_j at the jet section $x/D = 3$ for the groups of turbulent and transitional jets. It is evident in Fig. 13(a) that a coflow increases the turbulence intensity of a turbulent jet even inside ZFE. However, for a transitional jet, turbulence intensity inside ZFE is only slightly increased by presence of a coflow (Fig. 13b). The turbulence intensities u'/U_j of our transitional jets inside ZFE are obviously lower than those of the turbulent jets but Fig. 11 shows that in the downstream ZEF, the turbulence intensities u'/U_{ec} of the transitional jets become higher than the turbulent jets. This may be due to the faster rate of drop of centerline jet excess velocity in the ZEF of transitional jets (Fig. 5).

For the scalar field, the level of concentration fluctuations at a point in the jet is statistically measured by the standard deviation of concentration fluctuations, c' , as defined by:

$$c' = \sqrt{\frac{1}{T} \int_0^T (C(t) - C)^2 dt} \quad (8)$$

where C is the mean concentration at that point, $C(t)$ is the instantaneous concentration at time t , and T is the measurement duration. Fig. 14 shows the radial profiles of concentration fluctuation levels inside the ZFE when a coflow at different R is present. The jet sections shown are inside the ZEF listed in Table 3. Unlike the turbulence intensity data in Fig. 13, presence of a coflow leads to obvious increases in c'/C_j in the transitional and laminar jets but has little effects on the turbulent jets. Our turbulence properties inside ZFE presented in Figs. 13-14 show some interesting but inconclusive observations. The different observations on turbulent velocity and scalar properties inside the ZFE need further investigations.

On reaching the ZEF, the jet is approaching self-similarity. The normalized radial profiles of c'/C_c against r/b_T are shown in Fig. 15 for our simple jets at different Re . The profiles in the turbulent jet at $x/D = 35, 45$ and 55 show reasonably good self-similarity. The profiles are double-peaked with peak levels of fluctuations reaching $c'/C_c \approx 0.25$ and located at $r/b_T \approx \pm 1$. The results are in agreement with the similarity profiles measured by Papanicolaou and List (1988) and Webster et al. (2001) for high Re simple jets at $x/D > 40$. In Fig. 15, the profiles of c'/C_c for the transitional jet lie above those of the turbulent jet with peak values of c'/C_c near 0.3. The laminar jet has even higher peak values of $c'/C_c \approx 0.35$ with the self-similarity of profiles being the worst among the three jets.

When the jet is in a coflow, the self-similar behavior of radial profiles of c'/C_c become obviously poorer. Profiles at different jet sections are not shown but at $R > 0.2$, the profiles are found to keep on reaching higher peak values until our most downstream jet section at $x/D = 50$. Fig. 16 shows the normalized radial profiles of c'/C_c at the jet section $x/D = 50$. It is evident that for all the three groups of jets, a coflow of strength R about 0.2 or higher is found to raise the profiles to significantly higher values of c'/C_c inside the jet. The results of a turbulent jet and a transitional jet in coflow simulated by the towed jet experiments are included in Fig. 16. They generally agree with the results from the flume experiments.

5. Conclusions

We have carried out velocity and concentration measurements on a number of submerged round jets in a stagnant environment and in coflow using LDA and LIF. The test cases cover different values of jet Reynolds number Re and coflow velocity ratio R . Different flow behaviors are observed on jets at three different ranges of Re and the test cases are classified into initially laminar jets, transitional jets and turbulent jets. Spreading of the jet and dilution of jet effluent in the ZEF are investigated from the decay of mean velocity and mean concentration along the jet centerline and the development of radial profiles of mean velocity and concentration across successive sections of the jet.

The centerline velocity and concentration in ZEF of the simple jets drop with x . In all jets, the decay curves can be described reasonably well by the x^{-1} power law relationships provided that the data are adjusted with an appropriate virtual origin of the jet. The decay constant for the centerline velocity has a value 5.5 for the turbulent jets but the transitional and laminar jets have a lower value at 4.5. The virtual origin in the latter two groups of jets is located at a longer distance downstream of the physical jet exit. Thus, increasing shorter lengths of ZFE, as measured from the physical jet exit, are found for the three groups of jets with increasing Re ranges. In the simple jets, these ZFE lengths are about $L/D \approx 9$ in the initially laminar jets, $L/D \approx 7$ in the transitional jets and $L/D \approx 5.5$ in the turbulent jets. The ZFE lengths for concentration are generally shorter than those for velocity by $1D$ to $2D$. When a coflow is present, collapse of centerline mean flow quantities at different coflow strengths R can be achieved through the use of jet excess velocity or normalized dilution and the normalization of downstream distances with the length scale l_m . Presence of a coflow is found to shorten the ZFE length further.

Most radial profiles of mean velocity and concentration in ZEF of our simple jets and jets in coflow are found to exhibit self-similarity to the Gaussian distribution, but with more scatter in the initially laminar jets or transitional jets. In the simple jets, the momentum and concentration jet widths are found to increase linearly with x in the transitional and turbulent jets with slopes of values close to previously reported values. The growth of jet widths in the laminar jets is non-linear. For our transitional and turbulent jets in coflow, both jet widths grow first linearly with x at $x < l_m$. This is the same as previously reported studies in this region of strong jet flow. Our data do not extend to the region of weak jet flow at $x/l_m > 50$ where past studies have found a growth rate as $x^{1/3}$. For laminar

jets in coflow, jet widths are found not to increase linearly with x at $x < l_m$ but farther downstream, the growth is similar to that in the higher Re jets. This suggests that the coflow has an effect of erasing the initial exit conditions of the jets.

Data of statistical turbulence quantities including turbulence intensity, Reynolds shear stress and concentration fluctuation levels have been obtained. In ZEF of simple jets, radial profiles of these turbulence quantities, when normalized with the local velocity, excess velocity or concentration at jet centerline, can roughly be described by self-similar forms. For jets in coflow, self-similarity of radial profiles is less evidently observed. For velocity fluctuations, presence of a coflow always increases the turbulence levels inside ZEF of transitional jets. In turbulent jets, a weak coflow at $R < 0.2$ does not produce noticeable change in turbulence and shear stress levels but the levels are increased inside jets in stronger coflow. In simple jets, normalized levels of concentration fluctuations in ZEF are the lowest in turbulent jets, higher in transitional jets and even higher in laminar jets. Presence of a coflow is found to increase these levels in all three groups of jets. The increase becomes very significant in coflow at $R \geq 0.2$.

Turbulence properties inside ZFE show some interesting features. For turbulent velocity fluctuations, there are small differences in turbulence intensities inside ZFE of transitional jets being in a stagnant environment or in a coflow but a coflow is found to increase the turbulence intensities inside ZFE of turbulent jets. The opposite observation is made on levels of concentration fluctuations. Presence of a coflow does not appear to change concentration fluctuation levels inside ZFE of turbulent jets.

We believe that the results in this paper supplement the database of mean flow behaviors of simple jets and jets in coflow, especially in the initial region where self-similarity of flow behavior has not been fully established. The data shed some light on the effect of initial exit jet Reynolds number and coflow velocity ratio.

Acknowledgments

The investigation is supported by a research grant (HKU 7517/03E) awarded by the Research Grants Council of Hong Kong. The authors wish to thank Mr. P. Liu for his assistance in carrying out some LDA measurements.

References

- Antoine, Y., Lemoine, F. and Lebouche, M. (2001). Turbulent transport of a passive scalar in a round jet discharging into a co-flowing stream. *Euro. J. Mech. B/Fluids*, 20, 275-301.
- Antonia, R. A., and Bilger, R. W. (1973). An experimental investigation of an axisymmetric jet in a coflowing air stream. *J. Fluid Mech.*, 61, 805-822.
- Babu, P. C., and Mahesh, K. (2004). Upstream entrainment in numerical simulations of spatially evolving round jets. *Phys. Fluids*, 16(10), 3699-3705.
- Burattini, P., Antonia, R. A., Rajagopalan, S., and Stephens, M. (2004). Effect of initial conditions on the near-field development of a round jet. *Exp. Fluids*, 37, 56-64.
- Chu, P. C. K., Lee, J. H. W., and Chu, V. H. (1999). Spreading of turbulent round jet in coflow. *J. Hydraul. Eng.*, 125(2), 193-204.
- Davidson, M. J., and Pun, K. L. (1999). Weakly advected jets in crossflow. *J. Hydraul. Eng.*, 125(1), 47-58.
- Davidson, M. J., and Wang, H. J. (2002). Strongly advected jet in a coflow. *J. Hydraul. Eng.*, 128(8), 742-752.
- Fischer, H. B., List, E. J., Koh, R. C. Y., Imberger, J., and Brooks, N. H. (1979). *Mixing in inland and coastal waters*, Academic Press, New York.
- Gaskin, S. J., Makernan, M. and Xue, F. (2004). The effect of background turbulence on jet entrainment: an experimental study of a plane jet in a shallow coflow. *J. Hydraul. Res.* 42, 531-540.
- Hussein, H. J., Capp, S. P., and George, W. K. (1994). Velocity measurements in a high-Reynolds-number, momentum-conserving, axisymmetric, turbulent jet. *J. Fluid Mech.*, 258, 31-75.
- Knudsen, M. (1988). Buoyant horizontal jets in an ambient flow. PhD thesis, University of Canterbury, New Zealand.
- Kwon, S. J., and Seo, I. W. (2005). Reynolds number effects on the behavior of a non-buoyant round jet. *Exp. Fluids*, 38, 801-812.
- Papanicolaou, P. N., and List, E. J. (1988). Investigation of round vertical buoyant jets. *J. Fluid Mech.*, 195, 341-391.
- Papantoniou, D., and List, E. J. (1989). Large-scale structures in the far field of buoyant jets. *J. Fluid Mech.*, 209, 151-190.

- Quinn, W. R. (2006). Upstream nozzle shaping effects on near field flow in round turbulent free jets. *Euro. J. Mech. B/Fluids*, 25, 279-301.
- Rajaratnam, N. (1976). *Turbulent jets*. Elsevier Scientific Publ. Co., Amsterdam, The Netherlands.
- Uddin, M. and Pollard, A. (2007). Self-similarity of coflowing jets: The virtual origin. *Phys. Fluids*, 19, 068103, 1-4.
- Webster, D. R., Roberts, P. J. W., and Ra'ad, L. (2001). Simultaneous DPTV/PLIF measurements of a turbulent jet. *Exp. Fluids*, 30, 65-72.
- Wood I. R., Bell, B. G., and Wilkinson, D. L. (1993). *Ocean disposal of wastewater, advanced series in ocean engineering, Vol. 8*, World Scientific, River Edge, N.J.
- Xu, G., and Antonia, R. A. (2002). Effect of different initial conditions on a turbulent round free jet. *Exp. Fluids*, 33, 677-683.
- Zarruk, G. A., Cowen, E. A. (2008). Simultaneous velocity and passive scalar concentration measurements in low Reynolds number neutrally buoyant turbulent round jets. *Exp. Fluids*, 44, 865-872.

TABLES

Table 1. Experimental Parameters for Velocity Measurements (along jet centerline and radial profiles*)

Initial exit condition	Reynolds number Re	Velocity ratio $R = U_o/U_j$	Coflow velocity U_o (m/s)	Jet exit velocity U_j (m/s)
Laminar	1,019	0	0	0.305
	1,027	0	0	0.307
Transitional	1,610*	0*	0	0.481
	1,655	0	0	0.495
	1,744	0	0	0.522
	2,509	0	0	0.750
Turbulent	3,270*	0*	0	0.978
	3,327	0	0	0.996
	3,405	0	0	1.020
	5,163	0	0	1.560
Laminar	1,060	0.026	0.009	0.317
	1,054	0.044	0.014	0.315
	1,043	0.049	0.015	0.312
	1,060	0.108	0.034	0.317
	1,054	0.279	0.088	0.315
	1,057	0.430	0.136	0.316
Transitional	1,592*	0.016*	0.008	0.476
	1,679*	0.054*	0.027	0.502
	1,669*	0.104*	0.052	0.499
	1,726*	0.192*	0.099	0.516
	1,692*	0.282*	0.143	0.506
Turbulent	3,334	0.008	0.008	0.997
	3,344	0.011	0.011	1.000
	3,251	0.036	0.035	0.972
	3,324	0.092	0.091	0.994
	3,378	0.121	0.122	1.010
	3,378*	0.050*	0.051	1.010
	3,458*	0.097*	0.092	1.034
	3,525*	0.203*	0.214	1.054

Table 2. Experimental Parameters for Concentration Measurements (towed jet experiments marked with *)

Initial exit condition	Reynolds number Re	Velocity ratio $R = U_o/U_j$	Coflow velocity U_o (m/s)	Jet exit velocity U_j (m/s)
Laminar	1,003	0	0	0.3
Transitional	1,672	0	0	0.5
Turbulent	3,345	0	0	1.0
	5,017	0	0	1.5
Laminar	1,003	0.055	0.017	0.3
	1,003	0.115	0.035	0.3
	1,003	0.200	0.060	0.3
	1,003	0.292	0.088	0.3
Transitional	1,672	0.049	0.025	0.5
	1,672	0.104	0.052	0.5
	1,672	0.198	0.099	0.5
	1,672	0.302	0.151	0.5
	1,672*	0.05*	0.025*	0.5
	1,672*	0.10*	0.050*	0.5
Turbulent	3,345	0.028	0.028	1.0
	3,345	0.050	0.059	1.0
	3,345	0.094	0.094	1.0
	3,345	0.199	0.199	1.0
	3,345*	0.05*	0.05*	1.0
	3,345*	0.08*	0.08*	1.0

Table 3. Parameters for Axial Development of Velocity and Concentration along Centerline of Simple Jets.

Initial exit condition of jet	Turbulent	Transitional	Laminar
Centerline velocity:			
Decay constant ($\sim x^{-1}$)	5.5	4.5	4.5
Virtual origin, x_0/D	0.0	2.5	4.5
ZEF length, L/D	5.5	7.0	9.0
\sim power of x (without x_0)	-1	-1.33	-1.5
Centerline concentration:			
Decay constant ($\sim x^{-1}$)	7.0	6.0	5.0
Virtual origin, x_0/D	-2.5	-0.5	4.5
ZEF length, L_T/D	4.5	5.5	9.5

Figure Captions

- Fig. 1 Mean velocity profiles near jet exit. (a) Turbulent jet at $Re = 3,405$; (b) transitional jet at $Re = 1,744$.
- Fig. 2 Decay of centerline velocity in simple jets. (a) Turbulent jets at $Re > 3,000$; (b) transitional jets at $Re \approx 1,600$ to $2,500$; (c) laminar jets at $Re \approx 1,000$ to $1,300$. Data at R numbers in brackets from Kwon and Seo (2005).
- Fig. 3 Downstream development of mean concentration along centerline of simple jets at different Reynolds numbers.
- Fig. 4 Downstream development of centerline velocity towards coflow velocity for jets in coflow. Groups of jets in the legends of R are laminar jets*, transitional jets and turbulent jets*.
- Fig. 5 Normalized decay of jet excess velocity along centerline of jets in coflow. (a) Turbulent jets: $Re \approx 3,300$; (b) transitional jets: $Re \approx 1,700$; (c) laminar jets: $Re \approx 1,100$.
- Fig. 6 Downstream development of normalized centerline dilution for jets in coflow. (a) Turbulent jets at $Re = 3,345$; (b) laminar jets* at $Re = 1,003$ and transitional jets at $Re = 1,672$. Velocity ratios in brackets are for towed jet experiments. Curves with slope $k = 0.16$ shown.
- Fig. 7 Self-similarity of radial profiles of mean velocity in ZEF. Gaussian distribution shown as solid curve. Jet sections are $x/D = \{8, 10, 12, 14, 16, 18, 20\}$. (a) Turbulent jets: $Re \approx 3,300$ to $3,500$; (b) transitional jets: $Re \approx 1,600$ to $1,700$.
- Fig. 8 Growth of momentum jet width of jets in coflow. Open symbols: transitional jets; filled symbol: turbulent jets*.

- Fig. 9 Growth of concentration width in simple jets. Legends denote Reynolds numbers of jets.
- Fig. 10 Growth of concentration jet width of jets in coflow. (a) Turbulent jets at $Re = 3,345$ and transitional jets* at $Re = 1,672$; (b) laminar jets at $Re = 1,003$. Velocity ratios in brackets are for towed jet experiments.
- Fig. 11 Normalized radial profiles of turbulence intensity in ZEF of transitional jets* and turbulent jets in coflow.
- Fig. 12 Normalized radial profiles of Reynolds shear stress in ZEF of transitional jets* and turbulent jets in coflow.
- Fig. 13 Effect of coflow on turbulence intensity inside ZFE. $x/D = 3$. (a) Turbulent jets; (b) transitional jets.
- Fig. 14 Effect of coflow on concentration fluctuation levels inside ZFE. (a) Turbulent jets, $x/D = 3$; (b) transitional jets, $x/D = 4$; (c) laminar jets, $x/D = 5$.
- Fig. 15 Radial profiles of concentration fluctuation levels in ZEF of simple jets. Open symbols at lower levels: turbulent jets at $Re = 3,345$; filled symbols: transitional jets at $Re = 1,672$; open symbols at higher levels: laminar jets at $Re = 1,003$.
- Fig. 16 Similarity of radial profiles of concentration fluctuation levels in ZEF. $x/D = 30$. (a) Turbulent jets at $Re = 3,345$; (b) transitional jets at $Re = 1,672$; (c) laminar jets at $Re = 1,003$. Velocity ratios in brackets are for towed jet experiments.

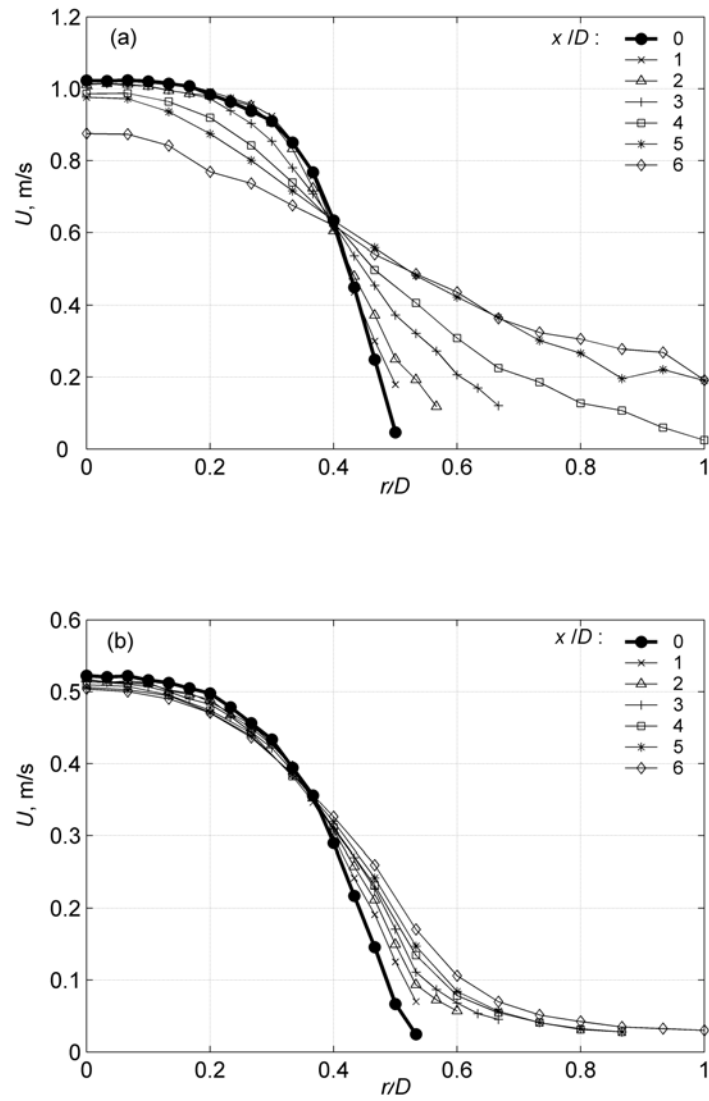


Fig. 1 Mean velocity profiles near jet exit. (a) Turbulent jet at $Re = 3,405$; (b) transitional jet at $Re = 1,744$.

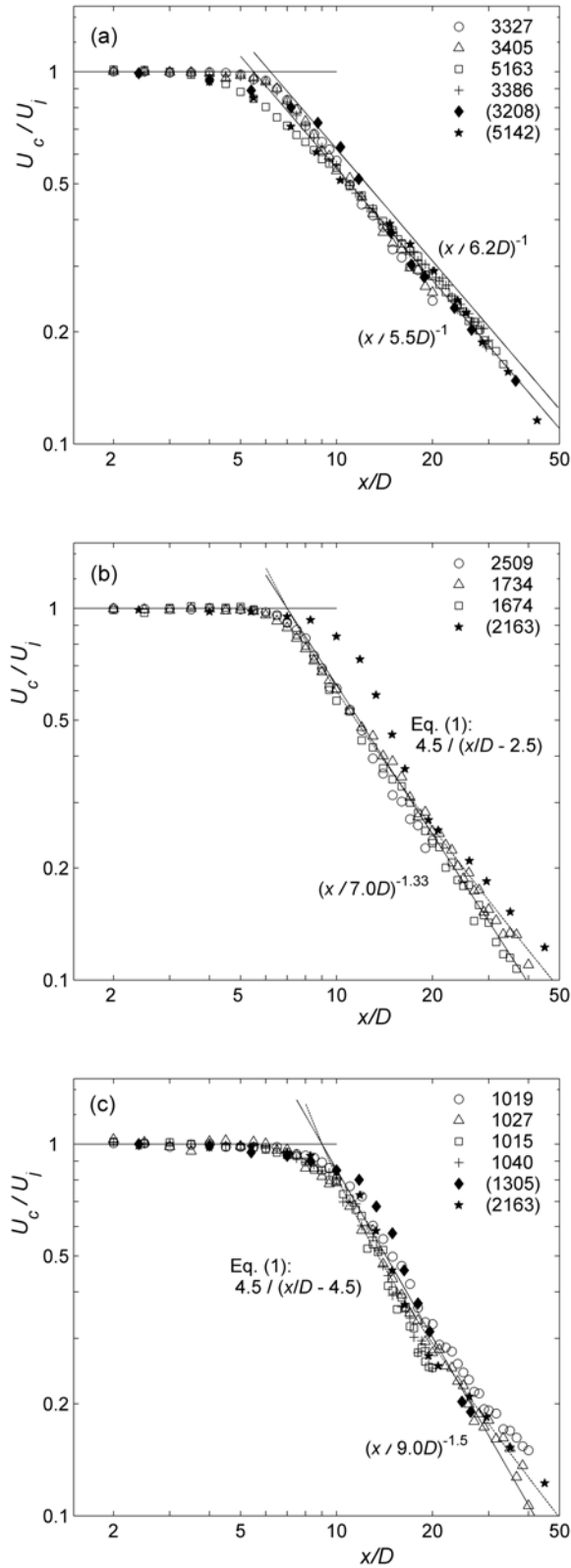


Fig. 2 Decay of centerline velocity in simple jets. (a) Turbulent jets at $Re > 3,000$; (b) transitional jets at $Re \approx 1,600$ to $2,500$; (c) laminar jets at $Re \approx 1,000$ to $1,300$. Data at Re numbers in brackets from Kwon and Seo (2005).

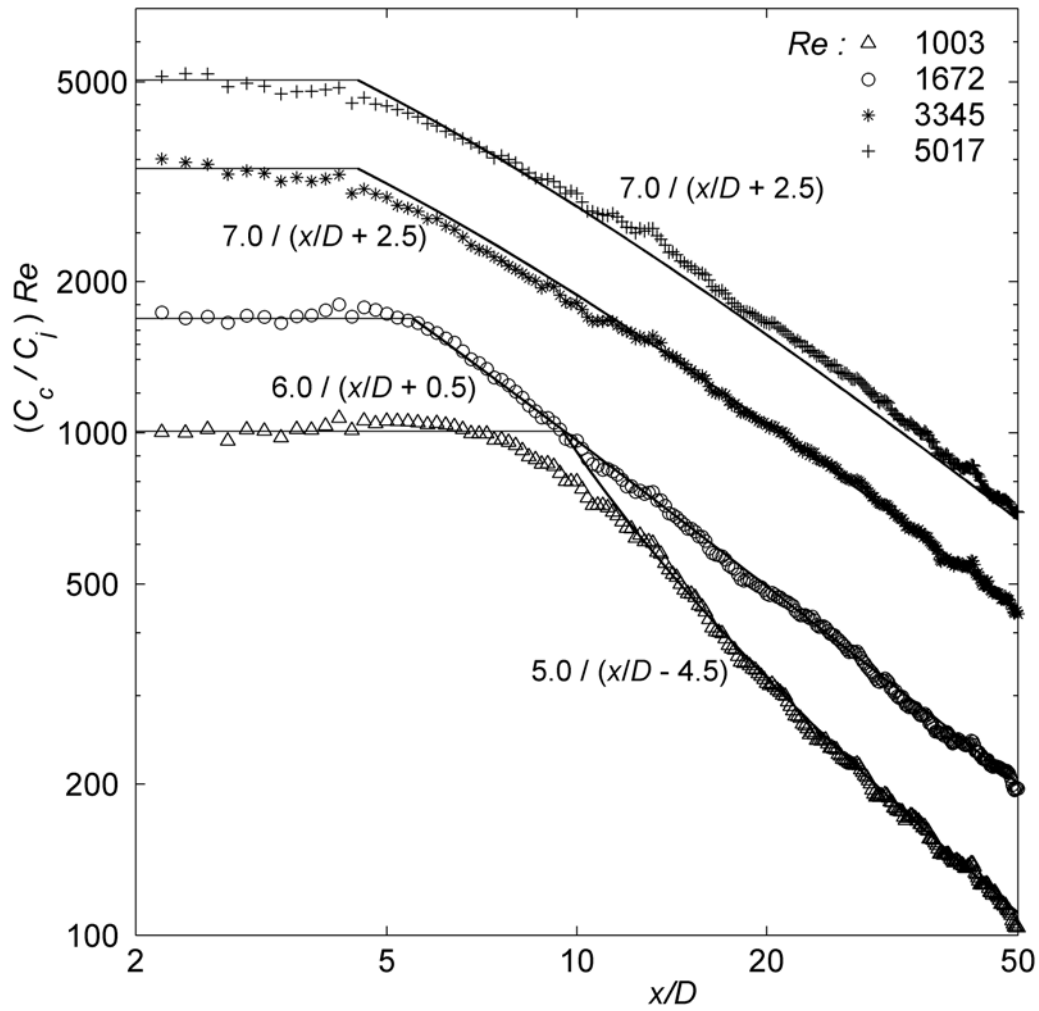


Fig. 3 Downstream development of mean concentration along centerline of simple jets at different Reynolds numbers.

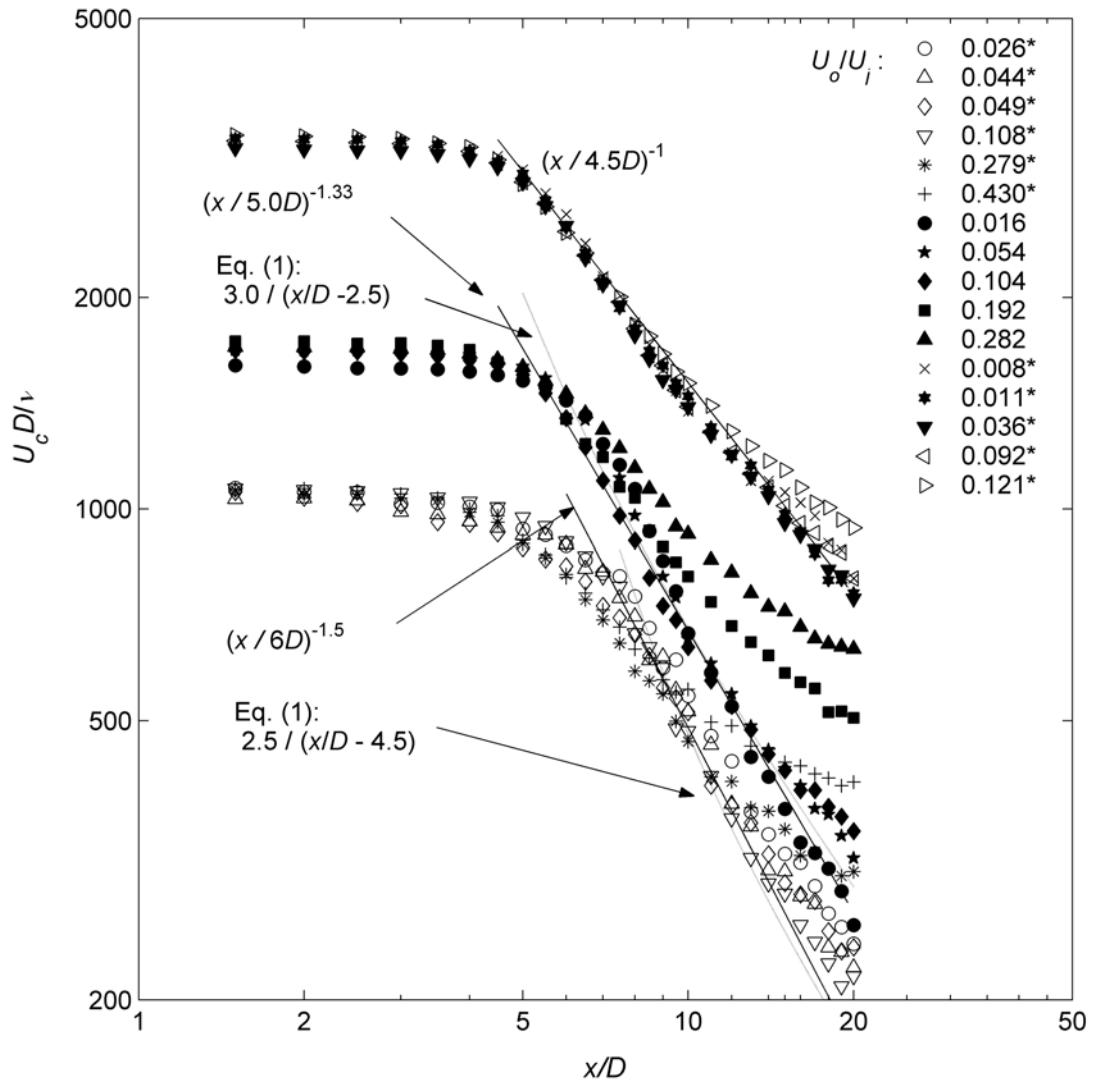


Fig. 4 Downstream development of centerline velocity towards coflow velocity for jets in coflow. Groups of jets in the legends of R are laminar jets*, transitional jets and turbulent jets*.

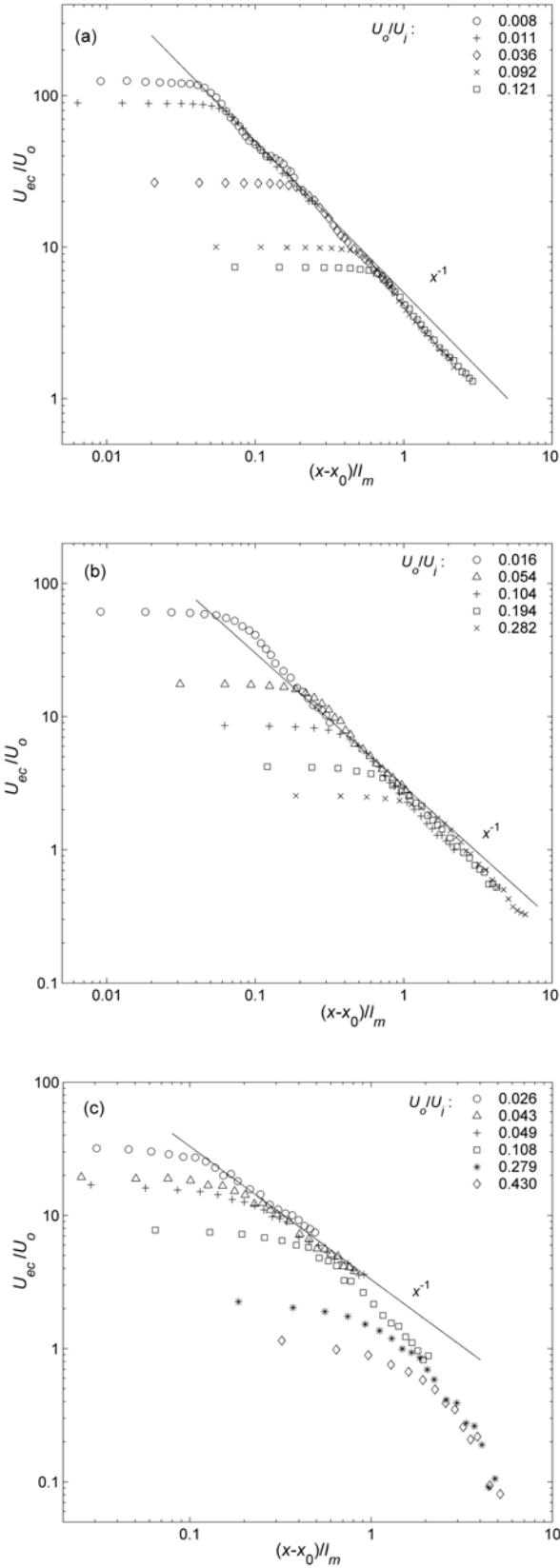


Fig. 5 Normalized decay of jet excess velocity along centerline of jets in coflow. (a) Turbulent jets: $Re \approx 3,300$; (b) transitional jets: $Re \approx 1,700$; (c) laminar jets: $Re \approx 1,100$.

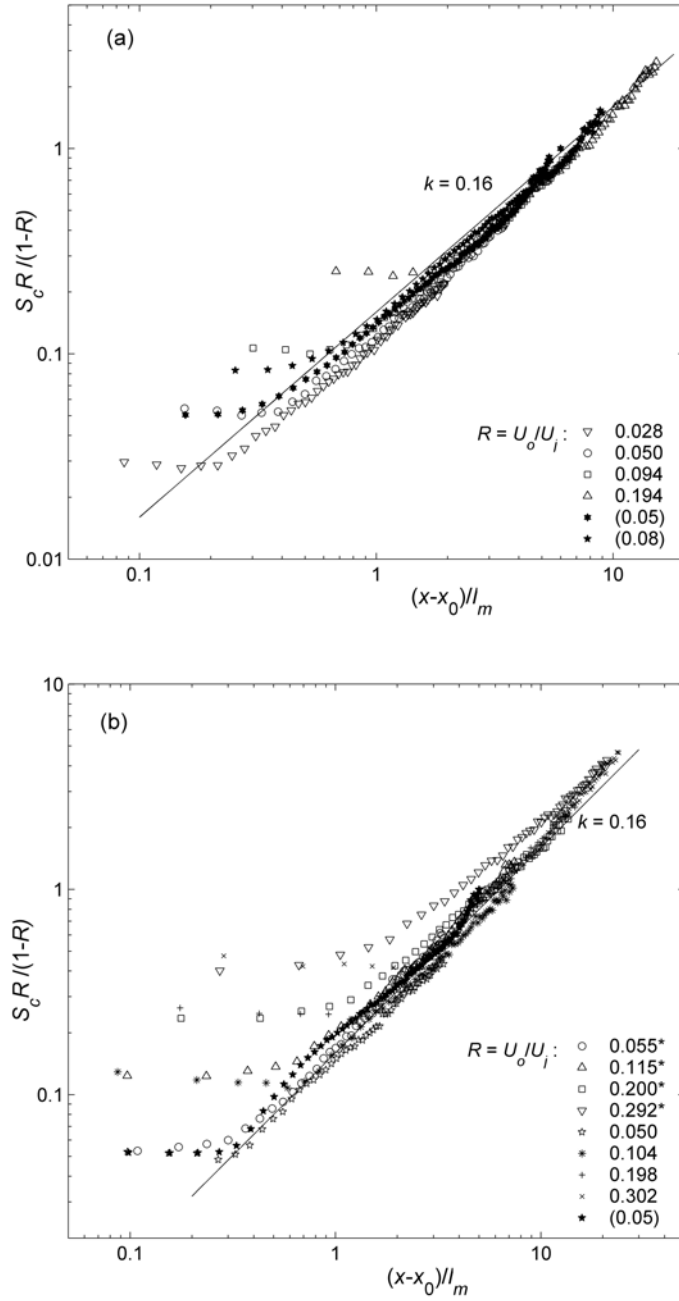


Fig. 6 Downstream development of normalized centerline dilution for jets in coflow. (a) Turbulent jets at $Re = 3,345$; (b) laminar jets* at $Re = 1,003$ and transitional jets at $Re = 1,672$. Velocity ratios in brackets are for towed jet experiments. Curves with slope $k = 1.6$ shown.

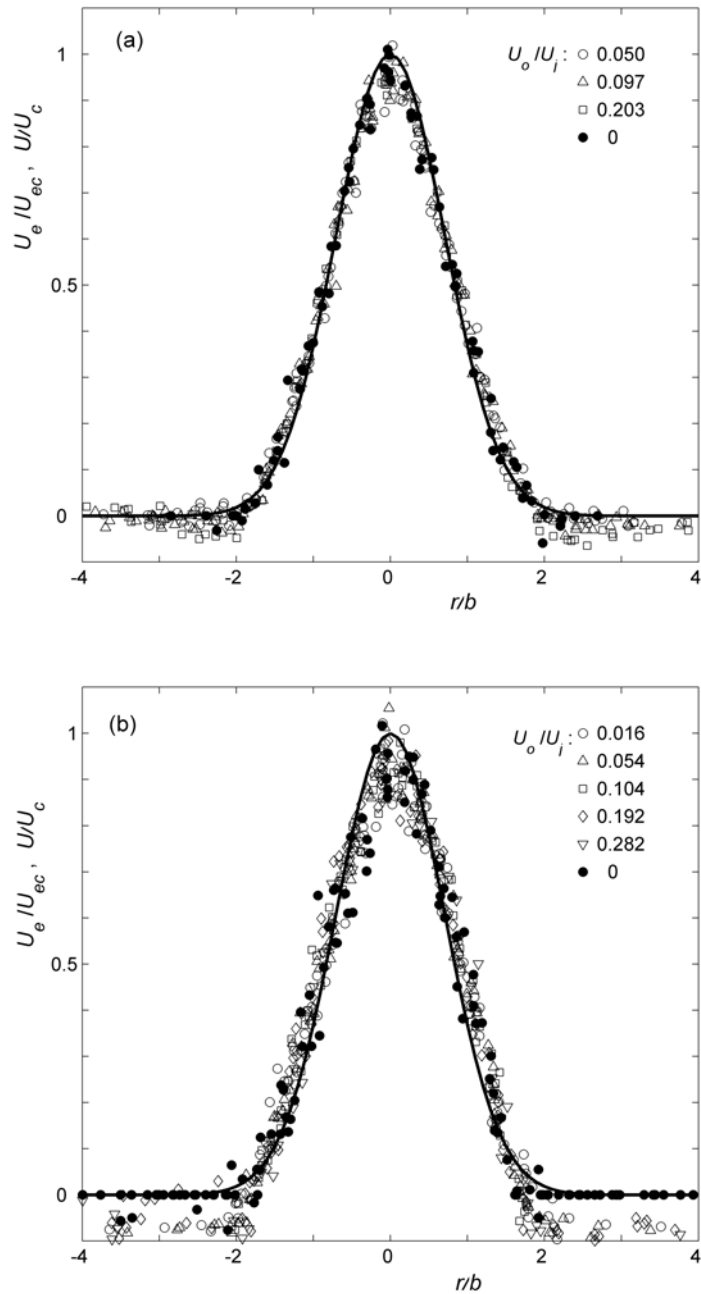


Fig. 7 Self-similarity of radial profiles of mean velocity in ZEF. Gaussian distribution shown as solid curve. Jet sections are $x/D = \{8, 10, 12, 14, 16, 18, 20\}$. (a) Turbulent jets: $Re \approx 3,300$ to $3,500$; (b) transitional jets: $Re \approx 1,600$ to $1,700$.

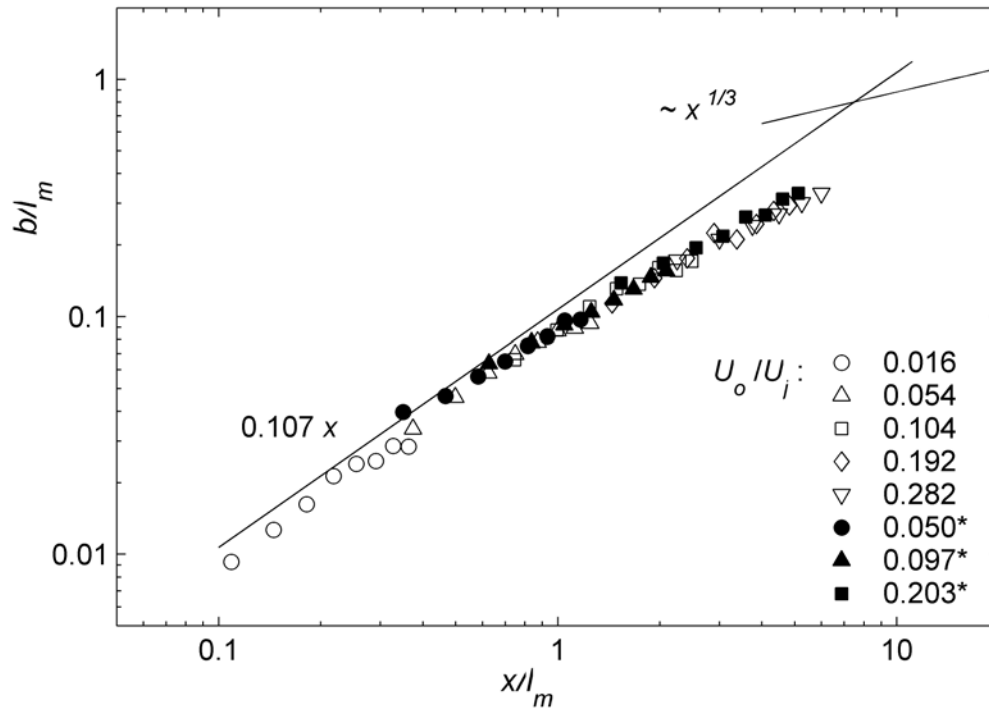


Fig. 8 Growth of momentum jet width of jets in coflow. Open symbols: transitional jets; filled symbol: turbulent jets*.

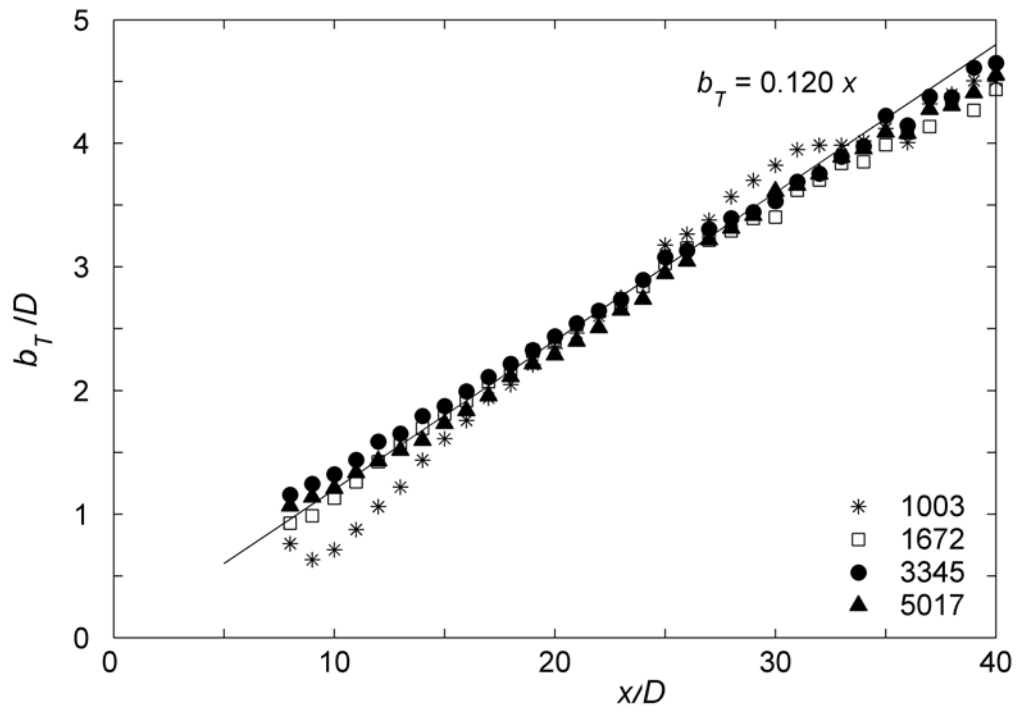


Fig. 9 Growth of concentration width in simple jets. Legends denote Reynolds numbers of jets.

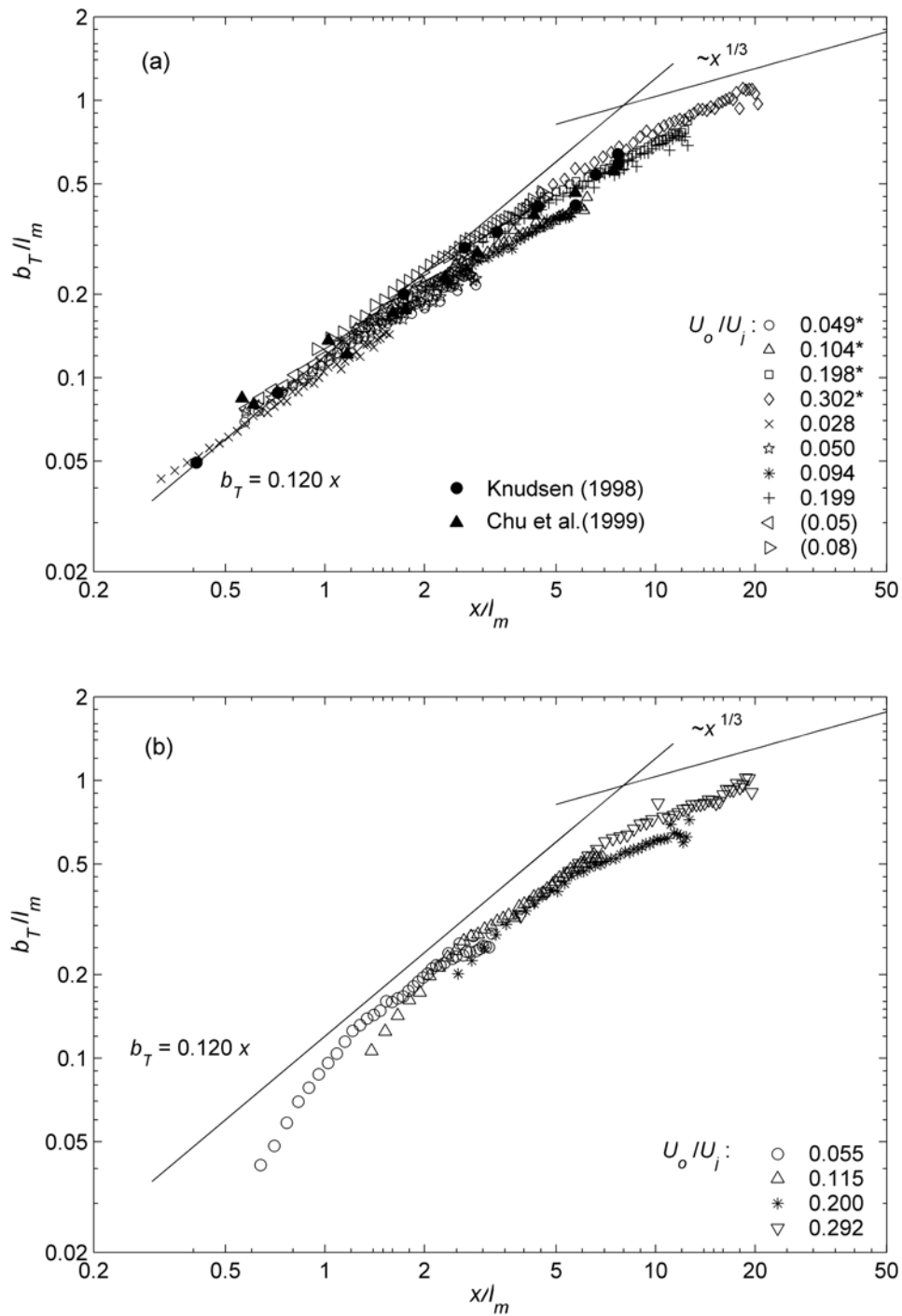


Fig. 10 Growth of concentration jet width of jets in coflow. (a) Turbulent jets at $Re = 3,345$ and transitional jets* at $Re = 1,672$; (b) laminar jets at $Re = 1,003$. Velocity ratios in brackets are for towed jet experiments.

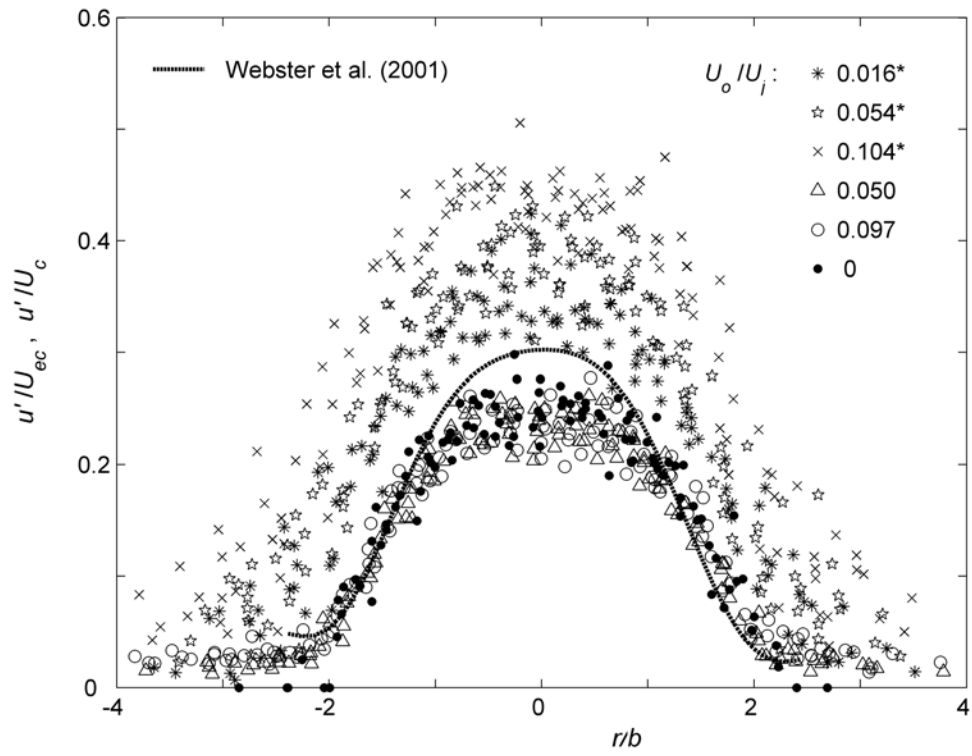


Fig. 11 Normalized radial profiles of turbulence intensity in ZEF of transitional jets* and turbulent jets in coflow.

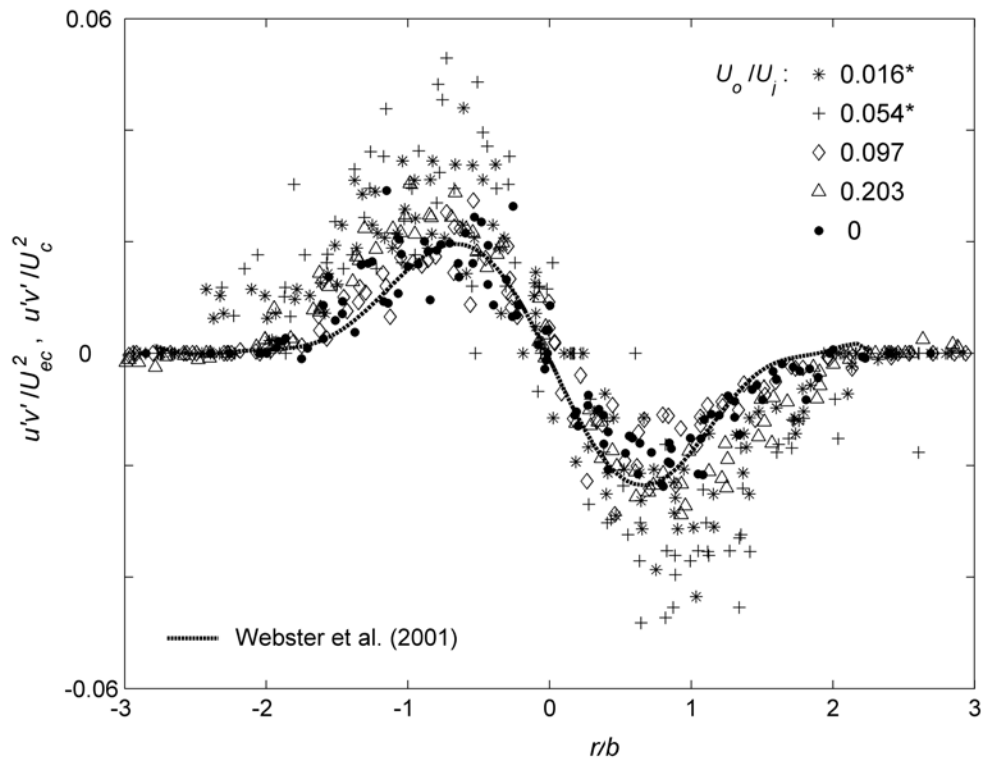


Fig. 12 Normalized radial profiles of Reynolds shear stress in ZEF of transitional jets* and turbulent jets in coflow.

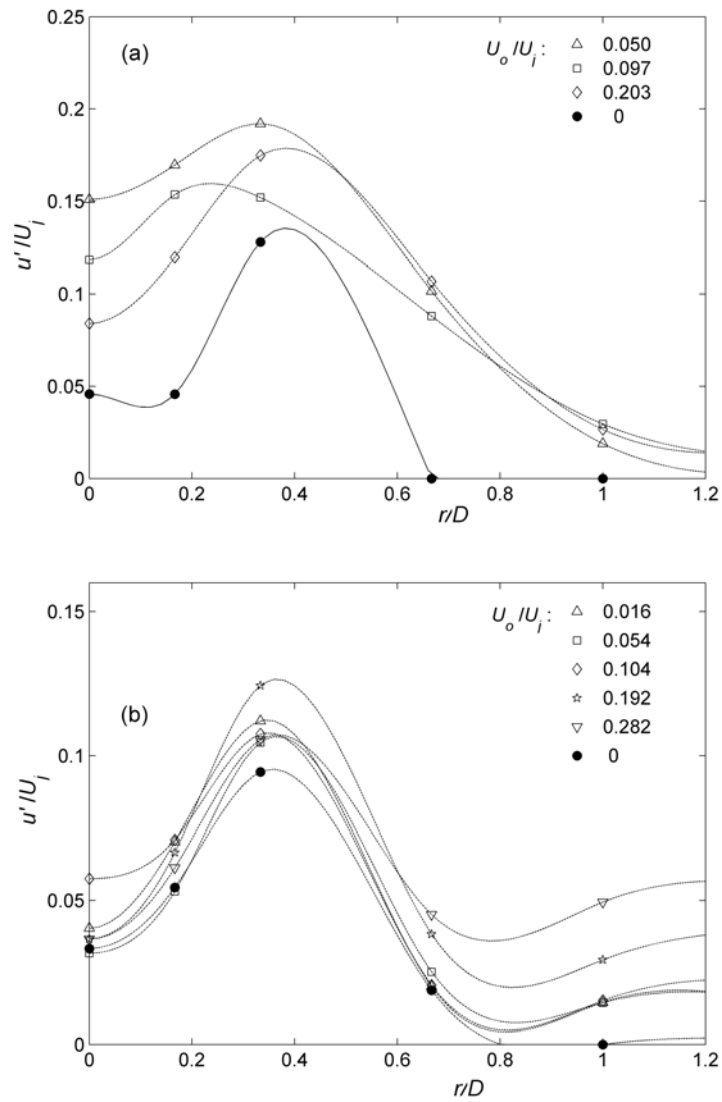


Fig. 13 Effect of coflow on turbulence intensity inside ZFE. $x/D = 3$. (a) Turbulent jets; (b) transitional jets.

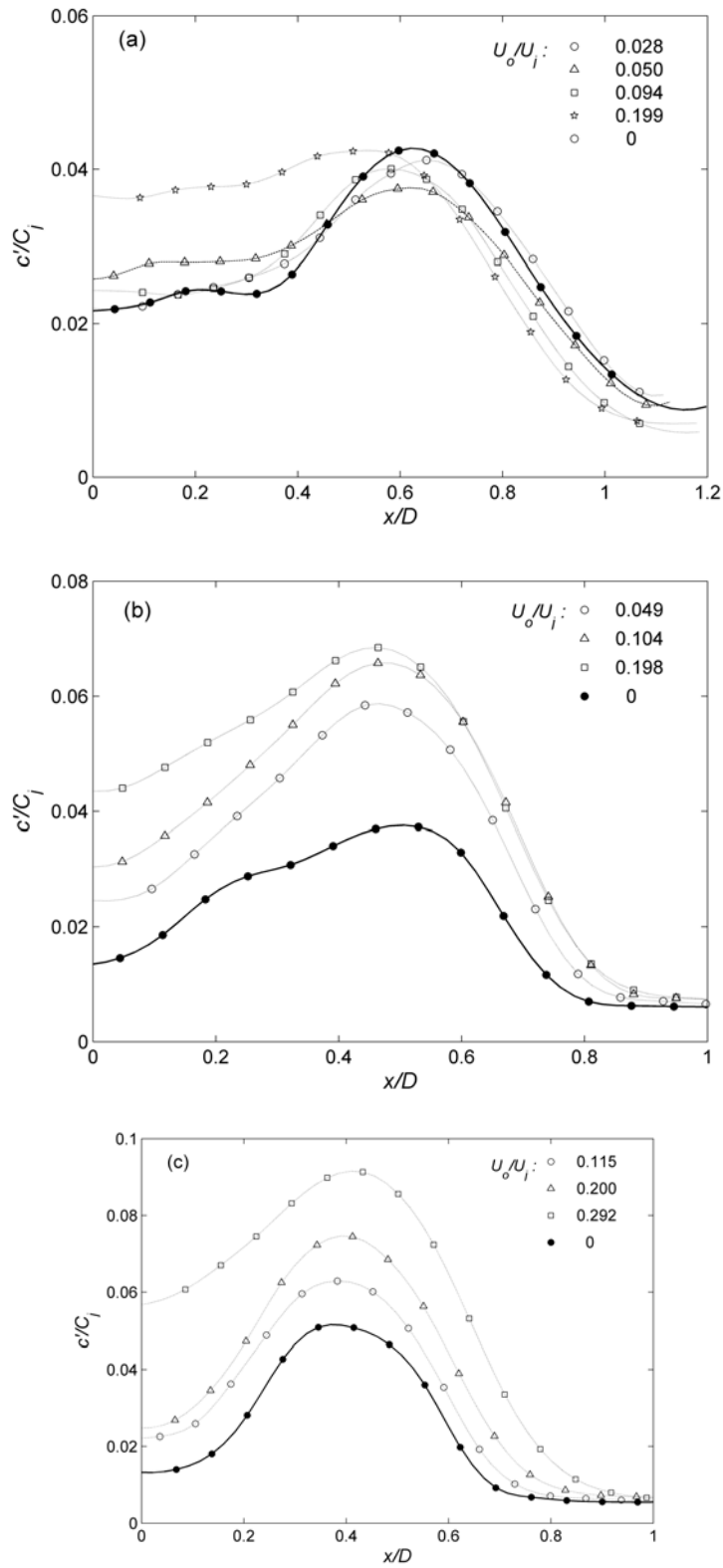


Fig. 14 Effect of coflow on concentration fluctuation levels inside ZFE. (a) Turbulent jets, $x/D = 3$; (b) transitional jets, $x/D = 4$; (c) laminar jets, $x/D = 5$.

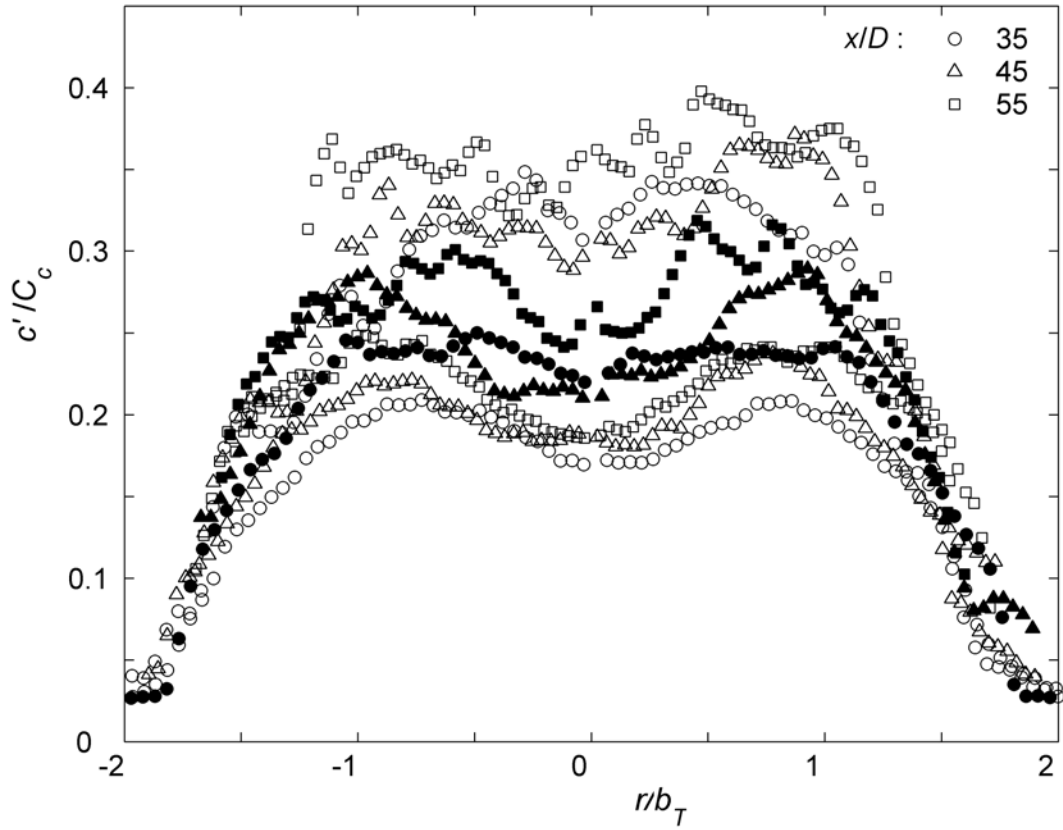


Fig. 15 Radial profiles of concentration fluctuation levels in ZEF of simple jets. Open symbols at lower levels: turbulent jets at $Re = 3,345$; filled symbols: transitional jets at $Re = 1,672$; open symbols at higher levels: laminar jets at $Re = 1,003$.

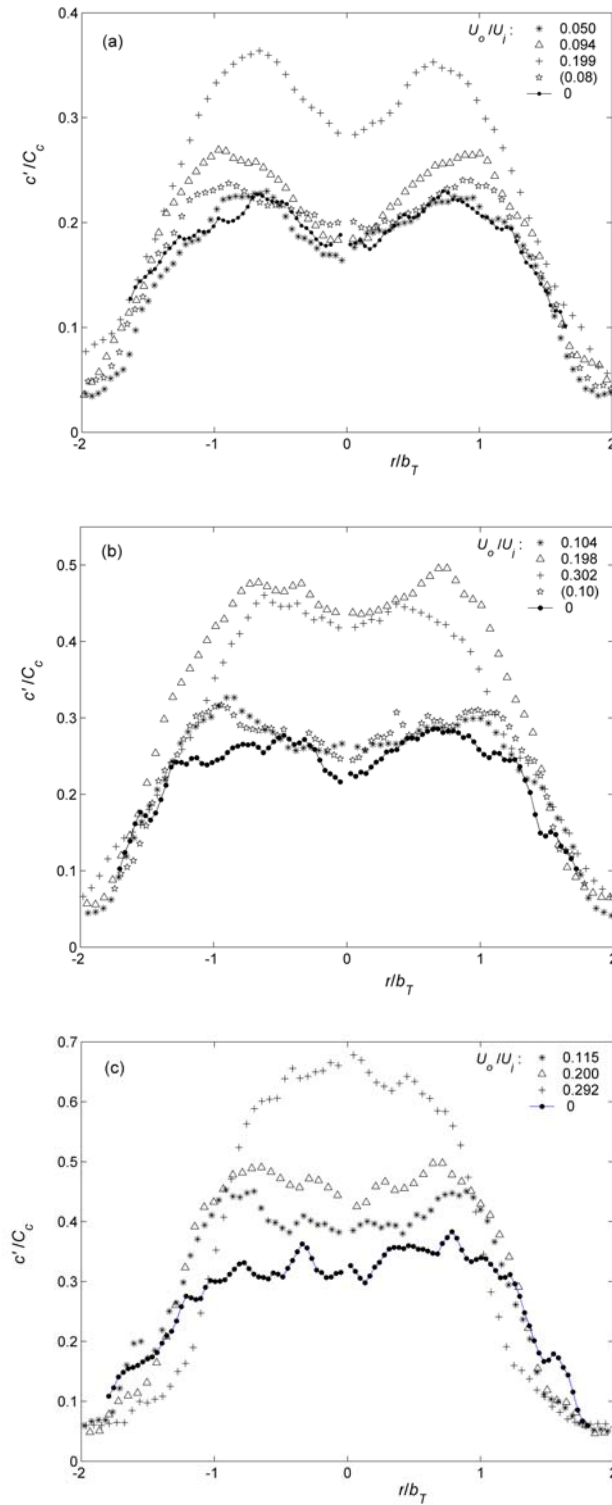


Fig. 16 Similarity of radial profiles of concentration fluctuation levels in ZEF. $x/D = 30$. (a) Turbulent jets at $Re = 3,345$; (b) transitional jets at $Re = 1,672$; (c) laminar jets at $Re = 1,003$. Velocity ratios in brackets are for towed jet experiments.